Supporting information

Hole transport layer-free deep-blue OLED with outstanding colour purity and high efficiency

Fei Huang,[ab] Hongli Liu,*[ab] Wei Sun,[ab] Xianggao Li [ab] and Shirong Wang *[ab]

[a] Tianjin University, School of Chemical Engineering and Technology, Tianjin 300072, China

[b] Collaborative Innovation Center of Chemical Science and Engineering, Tianjin 300072, China

*Email: liuhongli@tju.edu.cn (H.L.).

*Email: wangshirong@tju.edu.cn (S.W.).

Content

1. Device fabrication and performance testing of OLEDs

MoO_3, N,N'-bis-(1-naphthyl)-N,N'-diphenyl-1,1'-biphenyl-4,4'-iamine (NPB), 1,3,5-tris(2-N-phenylbenzimidazolyl) benzene (TPBi), N,N'-Dicarbazolyl-3,5-benzene (mCP), 1,3,5-Tris(carbazol-9-ylphenyl)amine (TCTA) and Lithium fluoride (LiF) were purchased from Xi'an Polymer Light Technology Corp. Aluminum (Al, 99.999%) was obtained from Energy Chemical Technology Co. Ltd. Pentafluorobenzyl phosphonic acid (F_5BnPA) was purchased from Sigma-Aldrich. Other reagents were obtained from Tianjin Concord Technology Co. Ltd. Indium tin oxide (ITO) substrates (8 Ω/sq) were obtained from Advanced Election Tech.

ITO substrates were sonicated in detergent solution, deionized water, toluene, acetone and ethanol for 15 min, followed by boiling in ethanol. After drying with nitrogen, ITO substrates were treated with oxygen plasma cleaner at 80 W for 5 min to obtain cleaned ITO.

ITO substrates were immersed into 1 mM F_5BnPA/ethanol solution at 25±5 ℃ for 24 h to obtain F_5BnPA-ITO, which needs rinsing with ethanol and drying with nitrogen before use.

ITO substrates were placed in a common rotating sample holder in a vacuum chamber (5×10^{-4} Pa) for device fabrication. All the organic layers were deposited at a rate of 1-2 Å/s while the deposition rates for LiF, MoO_3 and aluminum were 0.1, 0.3 and 10 Å/s, respectively. The film thickness was monitored by a quartz thickness monitor.

The current−voltage characteristics of the devices were measured with a computer-controlled Keithley 2400 source meter. The brightness of the OLEDs was measured with a CS2000 Luminance Meter, together with color coordinates and emission spectra.

2. Device schematic and energy band diagram

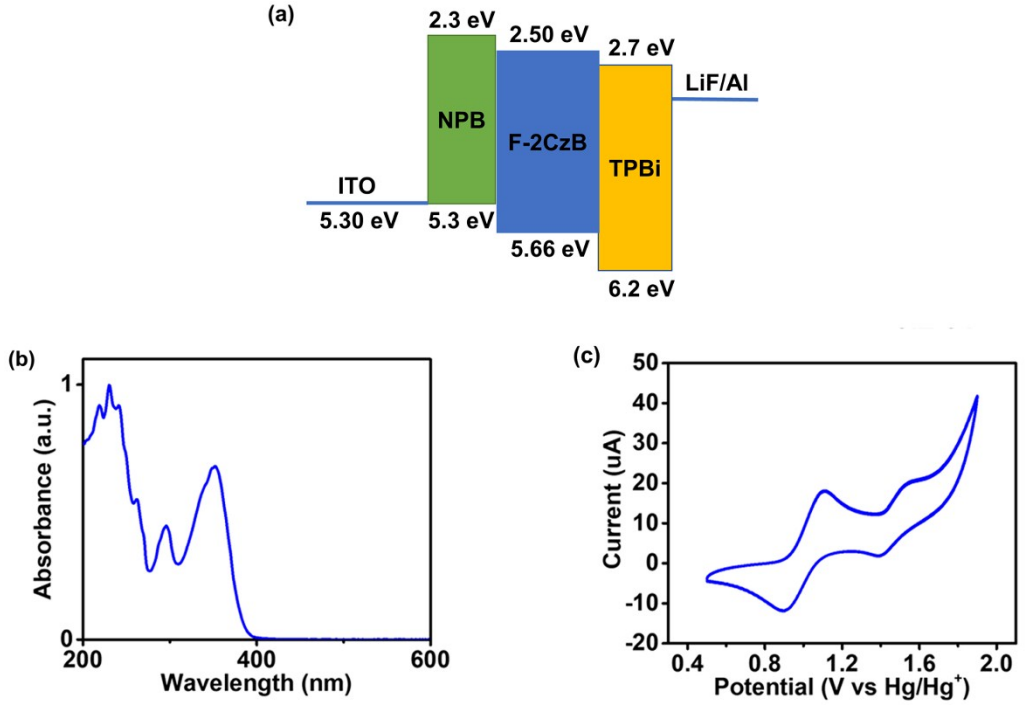

Fig. S1 (a) Device schematic and energy band diagram of NPB-OLED. (b) UV-vis absorption spectrum and (c) cyclic voltammetry curve of F-2CzB.

The optical band gap (E_g) of F-2CzB was 3.16 eV, determined by the onset absorption wavelength in CH_2Cl_2 solution (Figure S1d). Employing cyclic voltammetry (CV), the highest occupied molecular orbital (HOMO) energy level of F-2CzB was estimated to be -5.66 eV, according to the onset potential of oxidation (Figure S1e). Thus, the lowest unoccupied molecular orbital (LUMO) energy level of F-2CzB was -2.50 eV, calculated with HOMO energy level and E_g.

3. EL spectra and J-V characteristics of OLEDs

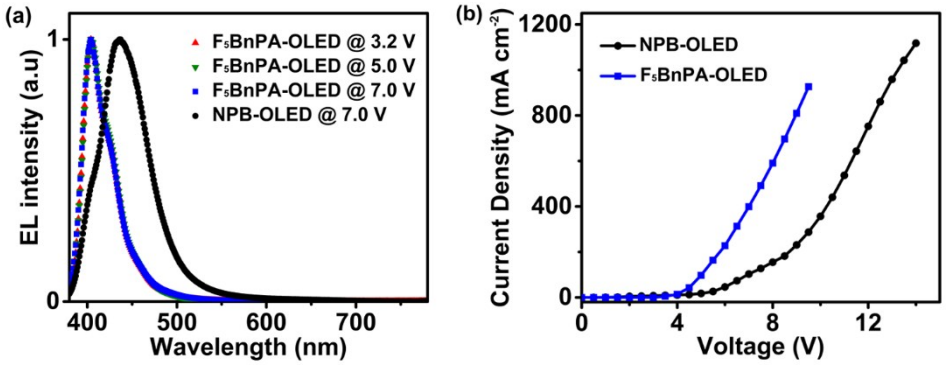

Fig. S2 (a) the EL spectra and (c) the current density-voltage (J-V) characteristics of F_5BPA -OLED and NPB-OLED.

4. Performance of deep-blue OLEDs ever reported

Performance of the F_5BnPA-OLED in this work and the deep-blue OLEDs ever reported with a CIEy not higher than 0.05 was summarized in Table S1.

Table S1 Performance of F_5BnPA-OLED and the deep-blue OLEDs ever reported.

Emitters	V_{on} [a] (V)	CIE [b]	FWHM [c] (nm)	EQE_{max} [d] (%)	Ref [e]
This work	**3.2**	**(0.162, 0.028)**	**38**	**4.43**	
DB1	3.9	(0.16, 0.04)		1.65	1
DB2	3.9	(0.16, 0.04)		2.48	1
mTPA-PPI	3.2	(0.161, 0.049)	47	3.33	2
DFPBI	3.0	(0.154, 0.042)	61	4.18	3
TPA-PIM		(0.161, 0.046)	35	3.28	4
TP-C-TP	6.76	(0.158, 0.045)	64	2.44	5
TP-C-TPB	6.56	(0.154, 0.042)	60	4.02	5
DIP	3.2	(0.158, 0.040)	44	3.27	6
TPAXAN	3.4	(0.154, 0.049)	49	4.62	7
DPACPhTPI	3.0	(0.156, 0.047)		3.50	8

[a] Voltage at 1 cd m^{-2}. [b] CIE coordinates of EL spectra. [c] Full width at half maximum. [d] Maximum external quantum efficiency. [e] References.

5. Carrier mobility of F-2CzB

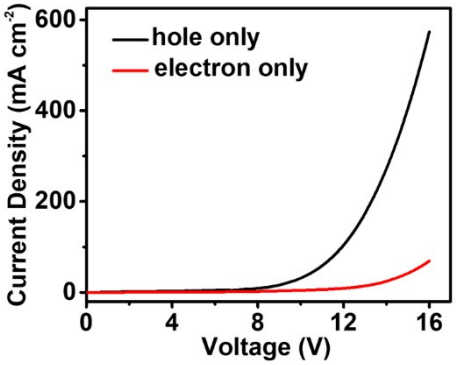

Fig. S3 The current density-voltage (J-V) characteristics of hole-only device and electron-only device with the configuration of ITO/NPB(15 nm)/F-2CzB(30 nm)/NPB(15 nm)/Al(100 nm) (**hole-only device**) and ITO/TPBi(15 nm)/F-2CzB(30 nm)/TPBi(15 nm)/LiF(1 nm)/Al(100 nm) (**electron-only device**)

6. Properties of ITO and F_5BnPA-ITO

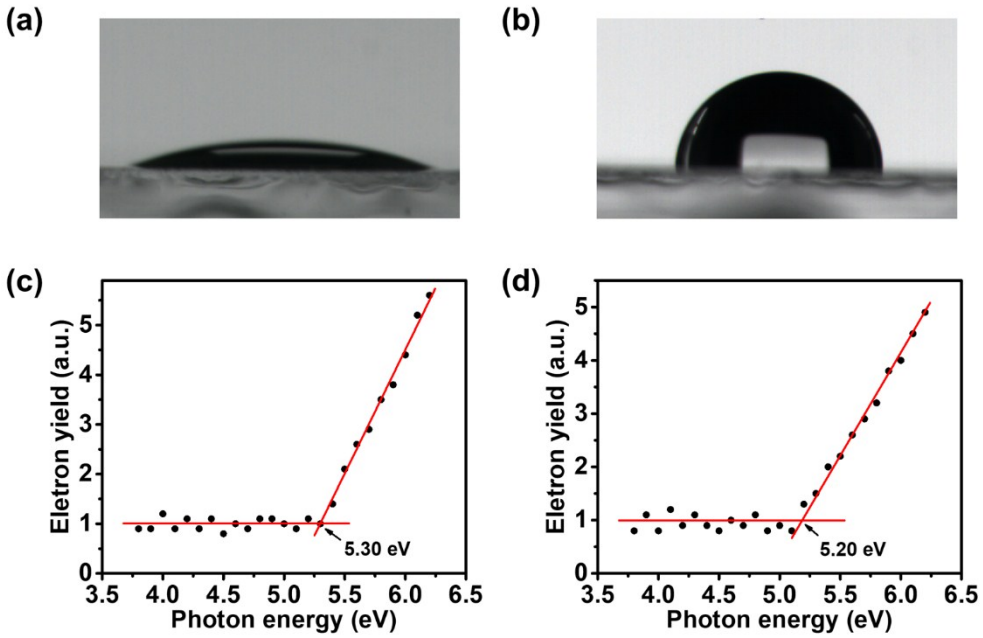

Fig. S4 Photographs of water contact angle for (a) ITO treated with oxygen plasma and (b) F_5BnPA-ITO. The work function of (c) ITO treated with oxygen plasma and (d) F_5BnPA-ITO.

7. Investigation on doped OLEDs

Doped OLEDs based on F-2CzB were fabricated, and the performance was investigated and compared with non-doped OLEDs (F_5BnPA-OLED and NPB-OLED with NPB layer of 5 nm). The device structures of the OLEDs are as follow:

Device A: F_5BnPA-ITO/F-2CzB(30 nm)/TPBi(15 nm)/LiF(1 nm)/Al(100 nm) (F_5BnPA-OLED)

Device B: F_5BnPA-ITO/F-2CzB: mCP(10 wt%, 30 nm)/TPBi(15 nm)/LiF(1 nm)/Al(100 nm)

Device C: ITO/NPB(5 nm)/F-2CzB(30 nm)/TPBi(15 nm)/LiF(1 nm)/Al(100 nm) (NPB-OLED with NPB film of 5 nm)

Device D: ITO/NPB(5 nm)/TCTA(5 nm)/F-2CzB: mCP(10 wt%, 30 nm)/TPBi(15 nm)/LiF(1 nm)/Al(100 nm)

Device schematic and energy band diagram of the doped OLEDs are shown in Fig. S5a and S5b, mCP (Fig. S5c) was adopted as host material. From the electroluminescence (EL) spectra in Fig. S5d and the EQE-current density characteristics in Fig. S5e, Device B obtained more excimer emission and lower EQE than Device A, Device D also showed more excimer emission and lower EQE than Device C. To investigate the reason for the poor performance of the doped OLEDs, doped films of F-2CzB: mCP (5, 10 and 15 wt%, 30 nm) and pure F-2CzB film (30 nm) were prepared, and the photoluminescence (PL) spectra were measured. As shown in Fig. S5f, regrettably, excimer in doped film was not intensively suppressed, which means that the doped emitting layers (EMLs) cannot make a great contribution to the suppression of excimer emission in the doped OLEDs. Additionally, compared with the highest occupied molecular orbital (HOMO) energy level F-2CzB (5.66 eV), the deeper HOMO energy level of mCP (5.8 eV) tends to bring about lower hole injection into the doped EMLs, which resulted in poor carrier balance in doped OLEDs and thus increased excimer emission and aggravated efficiency.

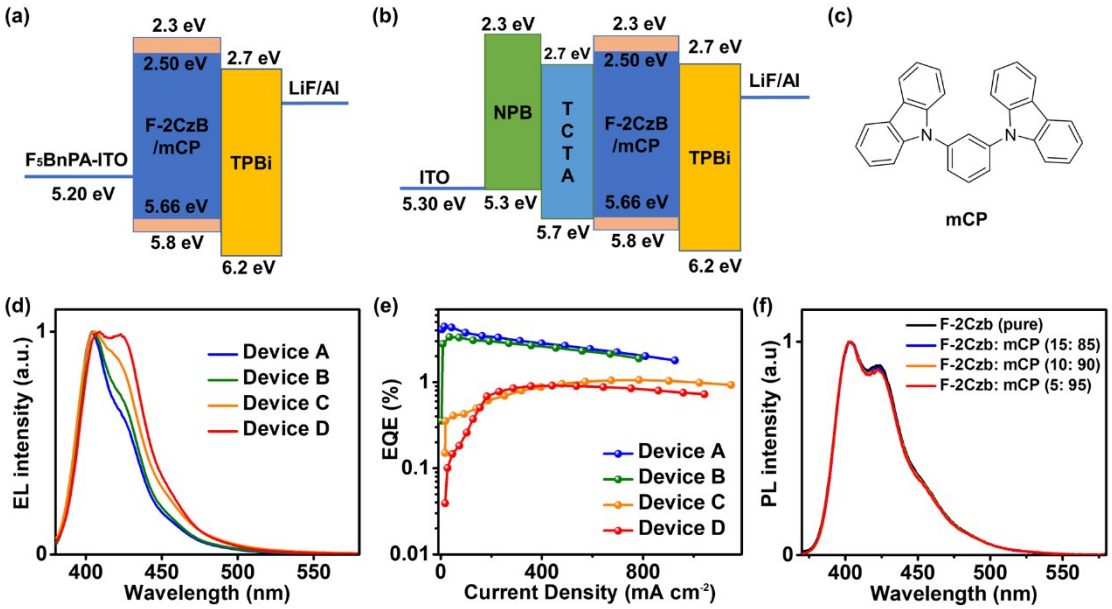

Fig. S5 Device schematic and energy band diagram of (a) Device B and (b) Device D. (c) Molecular structure of mCP. (d) EL spectra at 10 mA cm^{-2} and (e) EQE-current density characteristics of the devices. (f) PL spectra of pure F-2CzB film and doped film of F-2CzB: mCP (5, 10 and 15 wt%, 30 nm).

8. References

(1) Xu, H. X.; Sun, P.; Wang, K. X.; Li, J.; Wang, F.; Miao, Y. Q.; Wang, H.; Xu, B. S.; Wong, W. Y. Bipolar hosts and non-doped deep-blue emitters (CIE_y = 0.04) based on phenyl carbazole and 2-(2-phenyl-2H-1,2,4-triazol-3-yl)pyridine groups, *J. Mater. Chem. C* **2017**, *5*, 4455-4462.

(2) Liu, H. C.; Bai, Q.; Yao, L.; Zhang, H. Y.; Xu, H.; Zhang, S. T.; Li, W. J.; Gao, Y.; Li, J. Y.; Lu, P.; Wang, H. Y.; Yang, B.; Ma, Y. G. Highly efficient near ultraviolet organic light-emitting diode based on a meta-linked donor–acceptor molecule. *Chem. Sci*. **2015**, *6*, 3797-3804.

(3) Chen, S.; Lian, J. R.; Wang, W. G.; Jiang, Y.; Wang, X. D.; Chen, S. M.; Zeng, P. J.; Peng, Z. C. Efficient deep blue electroluminescence with CIEy ∈ (0.05–0.07) from phenanthroimidazole acridine derivative hybrid fluorophores. *J. Mater. Chem. C* **2018**, *6*, 9363-9373.

(4) Li, W. J.; Yao, L.; Liu, H. C.; Wang, Z. M.; Zhang, S. T.; Xiao, R.; Zhang, H. H.;

Lu, P.; Yang, B.; Ma, Y. G. Highly efficient deep-blue OLED with an extraordinarily narrow FHWM of 35 nm and a y coordinate <0.05 based on a fully twisting donor–acceptor molecule. *J*. *Mater*. *Chem*. *C* **2014** *2*, 4733-4736.

(5) Shin, H. Y.; Jung, H. C.; Kim, B. J.; Lee, J. H.; Moon, J. W.; Kim, J. H.; Park, J. W. Highly efficient emitters of ultra-deep-blue light made from chrysene chromophores. *J*. *Mater*. *Chem*. *C* **2016**, *4*, 3833-3842

(6) Jeong, S. J.; Hong, J. I. Extremely deep-blue fluorescent emitters with $CIE_y \leq 0.04$ for non-doped organic light-emitting diodes based on an indenophenanthrene core. *Dyes and Pigments* **2017**, *144*, 9-16.

(7) Kim, R.; Lee, S.; Kim, K. H.; Lee, Y. J.; Kwon, S. K.; Kim, J. J.; Kim, Y. H. Extremely deep blue and highly efficient non-doped organic light emitting diodes using an asymmetric anthracene derivative with a xylene unit. *Chem*. *Commun*. **2013**, *49*, 4664-4666.

(8) Huang, Z.; Wang, B.; Zhang, Q.; Xiang, S. P.; Lv, X. L.; Ma, L. X.; Yang, B.; Gao, Y.; Wang, L. Highly twisted bipolar emitter for efficient non-doped deep-blue electroluminescence. *Dyes and Pigments* **2017**, *140*, 328-336.